Effect of Mechanical Loading on PLGA Biodegradation

Authors:

Devleena Samanta [a], John A. Koithan [a], Anastasia H. Muliana [a], Matt Pharr [a]

[a] J. Mike Walker '66 Department of Mechanical Engineering, Texas A&M University, College Station, Texas, USA

Abstract

Poly(lactic-co-glycolic) acid (PLGA) has been widely implemented in tissue engineering and drug delivery systems, stemming from its biocompatibility, controllable biodegradation, non-toxicity, non-immunogenicity, and tunable mechanical properties. PLGA exhibits a broad range of degradation times and modes, which can be finely tuned by adjusting various parameters, namely by altering the ratio of lactide and glycolide units, molecular weight, end group functionality, specimen geometry, processing temperature, and chemistry of the surrounding medium. To tailor the degradation profile, the in vitro profile should closely reflect the in vivo profile; however, the effects of mechanical loading coupled with hydrolysis on PLGA biodegradation are typically overlooked. To this end, this study investigates the combined effects of mechanical loading and hydrolysis at 37ºC on the changes in the chemical and physical properties of PLGA as it degrades with time. We found that after several days of combined loading and hydrolysis at 37ºC PLGA significantly creeps, whereas non-loaded (but hydrolyzed) specimens only slightly elongate after relatively long-term hydrolysis (~60 days). Despite this observation and perhaps counterintuitively, the hydrolyzed non-loaded samples exhibited faster degradation than hydrolyzed loaded samples. Additionally, our studies indicated the presence of bulk erosion in hydrolyzed non-loaded samples and surface erosion in hydrolyzed loaded samples. We also observed (only) physical ageing in control samples (loaded and non-loaded samples that were not immersed in PBS but exposed to 37ºC). Based on these observations, we discuss potential underlying mechanisms for the observed differences in the biodegradation behavior of PLGA specimens with and without mechanical loading.

Keywords

Tissue engineering; Biodegradable polymers; In vitro degradation, PLGA, Biomedical implants

1. Introduction

The biodegradable polymers poly(lactic acid) (PLA), poly(glycolic acid) (PGA), poly(lactic-co-glycolic acid) (PLGA), and polycaprolactone (PCL) represent a few of the most promising[1], FDA-approved materials used extensively in drug-delivery systems[2, 3], temporary tissue implants[4], regenerative medicine[5], and wound healing products like stents, sutures, staples, and meshes[6, 7]. In particular, implants minimize mechanical mismatch[8], which can result in muscle atrophy and stress-shielding[9], by gradually transferring stress to the healed tissues via matching the rate of regeneration of injured tissues to the degeneration rate of the implants. This approach enables tissue regeneration while eliminating the need for subsequent surgeries. Since these polymers generate products that are fully metabolized in the physiological medium, these implants are biocompatible, causing minimal physical irritation of tissues. They can also act as a drug reservoir by releasing the intended drug into the body as it erodes, which can facilitate the healing process.

Biodegradable polymers are subjected to hydrolysis of their functional groups in an aqueous medium, causing the intrusion of water into the bulk of the polymer, which results in the scission of polymeric chains and the production of new chain ends[10]. The original chains often keep breaking into smaller segments, constantly reducing the molecular weight. Once the chain lengths are small enough, they diffuse through the polymer surface as oligomers and monomers and can act as auto-catalysts for hydrolysis. Although the effect of hydrolysis itself can efficiently capture the degradation profile of drug delivery systems, in vivo these biodegradable polymers for implants are constantly subjected to concurrent mechanical loading and fluid sorption at body temperature, causing degradation through erosion. This erosion process can be highly unpredictable, and the slightest change in the environment, loading conditions, or polymer properties can impact the mode and rate of degradation.

Our primary goal in this manuscript is to establish how the erosion and degradation processes of the PLGA copolymer are impacted by mechanical loading during fluid sorption at human body temperature (37ºC). It has been previously established that implants should degrade via surface erosion (or heterogeneous erosion) rather than bulk erosion (or homogeneous erosion), because bulk erosion occurs throughout the entire volume of the implant, thereby engendering abrupt structural failure of the implants[11]. By contrast, surface-eroding polymers have a more predictable erosion process[12]. Unfortunately, there is a lack of comprehensive understanding of the causes of surface and bulk erosion due to the combined effect of mechanical loading, fluid sorption, and hydrolysis. Numerous studies have been conducted on the influence of fluid sorption at 37°C on the hydrolytic degradation profile of the PLGA polymers and their properties after degradation; however, most studies do not account for the combined effects of mechanical loading and fluid sorption during the hydrolytic process. This oversight leads to an incomplete understanding of the degradation profile of biodegradable polymer implants, as in the in vivo degradation profile mechanical loading effects are unavoidable. Knowledge of the influence of mechanical loading on this process is thus critical in maintaining the structural integrity of the implants, and thus proper tissue regeneration through the gradual transfer of stress to the healing tissues.

Limited studies have been conducted that examine the effects of mechanical loading on the degradation kinematics of bioabsorbable polymers[13-16] and PLGA[15, 17]. Through these studies, it has already been established that PLGA and other bioabsorbable polymers exhibit creep-like behavior under static tensile loads[18]. However, most of the existing studies on PLGA biodegradation that have attempted to correlate the effect of loading on biodegradation have only considered the effects of pre-loading, that is, the samples are subjected to a load before immersion rather than during the immersion and degradation process itself[15, 19, 20] or the effect of loading after it has been immersed in biological media[18]. There is one study by Dreher[21] which performed a comparative study of the effect of simultaneous hydrolysis and pre-

degradation creep, static loading, and no loading on the mechanical properties of injection-molded PLGA ASTM Type V tensile bars. Based on the data at two time points (6 and 12 weeks), Dreher[21] observed that the statically loaded samples exhibited delayed loss of molecular weight compared to unloaded specimens. While this study gives us a general, valuable idea about how PLGA acts when subjected to loading and hydrolysis, it is not comprehensive and does not reflect the underlying mechanisms because of the limited nature of the data. Namely, this study did not capture the hydrolytic processes and degradation evolution as a chemical process, that is, the underlying potential erosion mechanism, because only data from 6 and 12 weeks of degradation was investigated, which might provide hints as to general trends but is limited in terms of uncovering underlying mechanisms of degradation and erosion. Our study provides a more comprehensive understanding of the effects of concurrent mechanical loading and hydrolysis on PLGA at body temperature (37°C). Specifically, we discuss how loading can affect the water uptake, degradation product retention, copolymer composition, and consequently affect the mode of erosion and the rate of degradation. Another important aspect of our study is that the T_g (36.8 ± 0.5°C) of the used PLGA before immersion in phosphate buffer saline is very close to the immersion temperature, T (37°C). So, it gives us a better insight into how the polymer acts under static loading conditions when the immersion temperature is close to the T_g. It has been previously noted that the proximity of the test temperature to the T_g of the polymers, like PLA and PLGA, affects the degradation rate, behavior[22-24], mechanical properties[25], and drug release rate[26, 27]. The other previous studies for PLGA or PLA under mechanical loading have been done for $T>T_g$[21, 28, 29], compared to our study, in which the test temperatures are quite near T_g.

In another study, Meng[30] used polymer membranes to describe the relationship between tensile stress and the degradation of PLGA over 8 weeks at room temperature by examining changes in surface morphology and mechanical properties including tensile strength and elastic modulus. Through micrographs of the surface morphologies of PLGA before and after degradation, they also established that increasing the magnitude of loading increases the porosity of the samples. This study is quite insightful but again did not elucidate the underlying hydrolytic degradation process and the possible causes. Thus, overall, the investigation into the effects of mechanical loading on PLGA has been highly limited, and the evidence is often conflicting. Our study offers new insights into PLGA biodegradation as its focus on the effect of combined mechanical loading, fluid sorption, and hydrolysis at $T=T_g$ on the erosion rate; the causes of erosion; the changes in the physicochemical properties including the glass transition temperature (T_g), crystallinity, and molecular weight; and how these properties are correlated to the rate and mode of degradation (i.e., surface or bulk) over 70 days. By comprehensively investigating these factors, our research aims to provide a deeper understanding of the hydrolytic degradation process of biodegradable polymers, specifically PLGA, used in tissue implants (like bone graft materials in the form of scaffolds, femur defect repair, mandibular defect repair, drug delivery microspheres, injectable hydrogels for soft tissue repair, nerve regeneration conduits, resorbable sutures, and implants for sustained drug release in various areas like under the skin or the eye[22, 31-34]) thereby contributing to the development of more effective and durable implant materials. Being able to accurately predict the degradation profile of the polymer in the form of implants or potential drug carriers also aids in having precise control over the drug release kinetics, which is critical in optimizing the therapeutic outcomes and minimizing the side effects[35-37]. As such, our study potentially not only contributes to creating more durable implants but also in making them better drug carriers. In the results section, we will first state the results and the basic evident conclusions from the results. Later, in the discussion section, we discuss how the results are interlinked to each other and provide insight into the underlying mechanisms.

2. Materials and Methods

2.1. Material. Ester-terminated poly (lactic-co-glycolic acid) (PLGA) copolymers with lactic to glycolic mole percentage ratio of 85:15 were supplied by Bonding Chemical (TX, USA). The as-received copolymers were amorphous, transparent, and light-yellowish in color. The weight average molecular weight (M_w), number average molecular weight (M_n), and polydispersity index (*PDI*) were 72,000 g mol^{-1}, 46,000 g mol^{-1}, and 1.56, respectively, as per our testing. The inherent viscosity was 0.5 dL g^{-1}, as stated by the vendor. Phosphate buffered saline (PBS) was purchased in powdered form from Sigma Aldrich, where one pouch, when dissolved in one liter of distilled or deionized water, yielded 0.01 M phosphate-buffered saline (0.138 M NaCl; 0.0027 M KCl) with a pH of 7.4.

2.2. Processing. Rectangular prism samples were injection molded using a Thermo Scientific HAAKE Minijet Pro and a 60×10×1 mm mold. The samples were subjected to a melt injection temperature of 138ºC, a mold temperature of 52ºC, and an injection pressure of 710 psi. The injection and cooling times were kept at 20 seconds and 120 seconds, respectively. All the processing parameters were kept constant to eliminate the differences in properties due to different injection molding parameters. The injection-molded rectangular plates were further cut into 21×10×1 mm samples due to the limited space of the incubator (Memmert USA LLC, IN 110, 115V, 50/60Hz, maximum temperature range to 80°C) and to accommodate the maximum possible elongation of the samples.

2.3. In Vitro Hydrolytic Degradation. The 21×10×1 mm samples were immersed (n=6, per condition, per time point) in the phosphate-buffered saline (PBS) solution (57.3g/6L), pH 7.4. Four conditions were considered, in which two sets of immersed samples were stored in a thermostatic bath (37±1°C) for 10, 20, 30, 40, 50, 60, and 70 days in PBS, with one set under static mechanical loading of 7.5 kPa and another set under no mechanical loading. Out of the four sets, the other two sets were kept as control samples exposed to 37±1°C but without any immersion in a thermostatic bath for 30, 60, and 90 days. One set of control samples was kept under static mechanical loading of 7.5 kPa, and the other set was not subjected to any mechanical loading. All the samples were kept in an incubator at 37ºC and 90% humidity (Memmert USA LLC, IN 110, 115V, 50/60Hz, maximum temperature range to 80°C).

For the mechanically loaded specimens **(Figure 1),** to keep the samples under constant loading, each sample had a stainless-steel metal clip attached to each end of the sample. The samples were oriented along the length (21 mm), and the clips covered 8 mm on each end, leaving a 5 mm exposed length **(Figure 2)**. On the bottom clip, a calibrated weight was hung using a thin metal wire. The effective (uniaxial) stress on each mechanically loaded sample was 7.5 kPa. Each metal clip had a sponge coating to increase the friction between the grips and the sample, to avoid slipping, and to minimize the effect of localized gripping pressure on the sample. The upper clip was attached to a metal wire, which was attached to a suction hook on both sides of the wall of a container. Each container carried two wires, and each wire carried three loaded samples. 6 L of PBS, pH 7.4, was poured into the container, covering all six samples to the top. The distance between the top horizontal wire from which the samples were hung and the bottom of the container was kept at 240 mm. The samples were allowed to elongate under the combined effect of constant loading, fluid sorption, and hydrolysis until they reached the bottom of the container. No additional loading was applied after the samples reached the bottom of the container. The pH was constantly monitored using Orion Star A221 from Thermo Fisher Scientific and was maintained at 7.4 in all instances. In the case of no loading, the bottom clips and the weights were removed, and all the other parameters were kept the same.

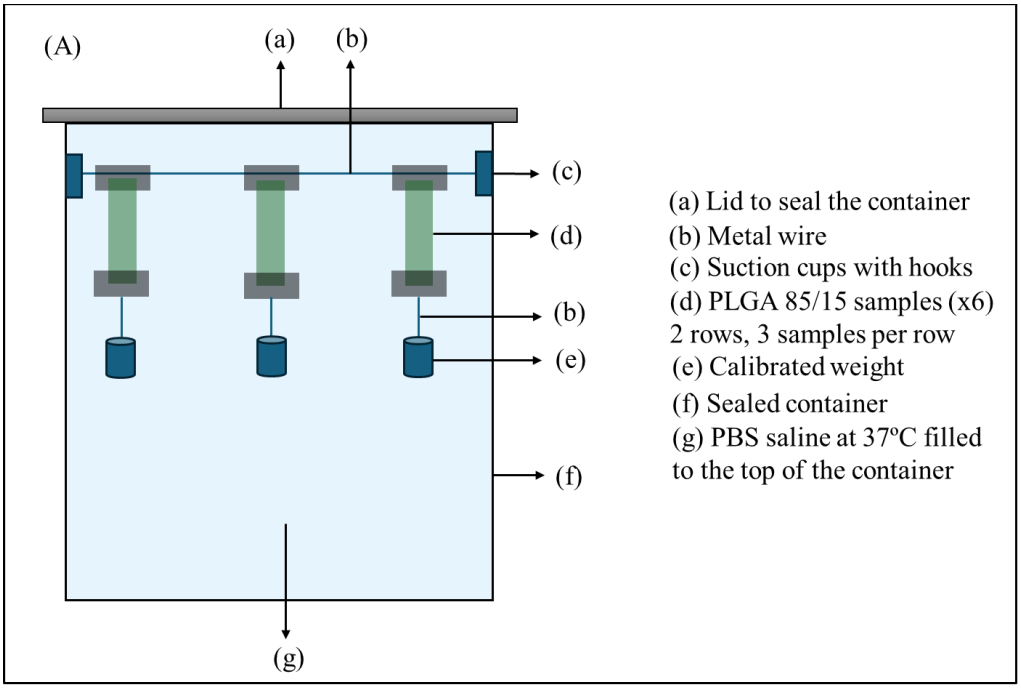

Figure 1. *Schematic of PLGA specimens under static mechanical loading of 7.5 kPa, undergoing hydrolytic degradation in-vitro. The specimens are maintained in PBS, and the entire set-up is housed in an incubator at 37ºC and 90% humidity.*

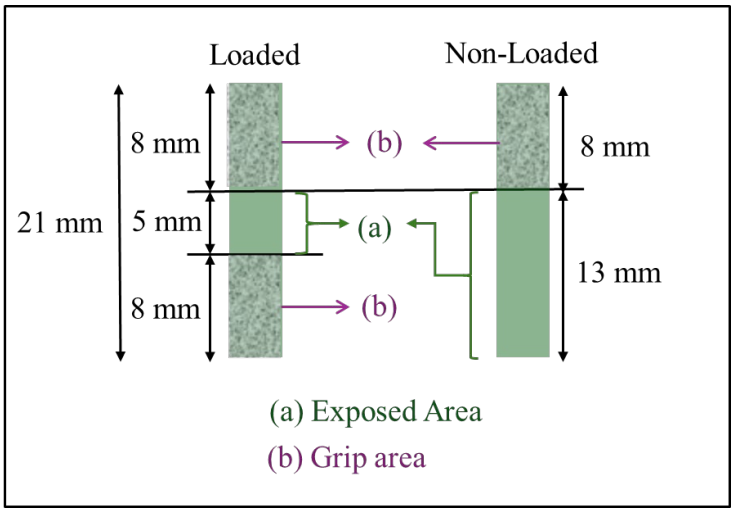

Figure 2. *Schematic of sample grip and exposed area for a loaded sample and non-loaded sample.*

2.4. Mass Calculation. Samples were weighed in their wet and dry states. For the wet state readings, the samples were pat-dried with soft tissues to absorb excess water and weighed immediately after being removed from the incubator. The samples were then placed in a desiccator for 72 hours (for comparative

weight measurements) at room temperature to dry, and the dried samples were weighed again. All the solutions were sieved to account for the samples that were too fragile to be retrieved otherwise.

2.5. Modulated Differential Scanning Calorimetry (MDSC). In conventional differential scanning calorimetry (DSC), to eliminate the influence of the thermal history of polymers, the glass transition temperatures (T_g) are typically measured during the second heating and cooling cycle. However, in this case, the results obtained from the second cycle may not mirror the reality of the PLGA co-polymer, where the effect of hydration inevitably changes after the first heating and cooling cycle. Moreover, if the sample is a mixture of two phases, as in the case after day 30 of degradation of PBS-immersed and non-loaded samples, the two phases can mix to form a single phase after melting. These phases might have vastly different thermal properties, leading to a complete degradation of one phase due to excessive heating, and hence a loss of information relevant to the hydrolytic process. Also, in the first heating scan, the enthalpy relaxation peak often overlaps with the glass transition, which convolutes the interpretation of the data.

As such, modulated temperature DSC (MDSC) experiments were conducted using a DSC 2500 from TA Instruments to determine the thermal properties (glass transition temperature, T_g; enthalpy of melting, ΔH_m) and %crystallinity. Temperature calibrations were performed using n-decane, indium, and tin standards. Indium was also used for enthalpy calibration. Sapphire of known heat capacity (C_p) was used for Tzero calibration. The results were obtained in a nitrogen atmosphere, using aluminum oxide as a standard. During the degradation process, the state of the material changes drastically; thus, both non-hermetically and hermetically sealed aluminum pans were used depending on the sample's morphology. The applied temperature range was also modified based on the sample's morphology to prevent damaging the DSC instrument. Since the glass transition temperature and enthalpy of melting depend on the ramp rate and sample size, the ramp rate was kept at 2ºC min^{-1} for all the sample conditions, using an average sample mass of 3.4 mg taken from the central region of the immersed specimens. The modulated temperature amplitude, modulation period, and ramp rate were 1ºC, 120 s, and 2ºC min^{-1}, respectively, and were kept constant for all the tests and degradation day points. The temperature range for the loaded samples in PBS and all the control samples was -20ºC to 150ºC. For the non-loaded samples, the temperature range was -20ºC to 150ºC until day 30 of degradation, followed by -90ºC to 60ºC until day 70 of degradation. The temperature range was changed due to the extreme changes in morphology in the non-loaded samples, i.e., the samples were liquidy, with PBS, and to avoid possible damage to the instrument.

2.6. Gel Permeation Chromatography (GPC). The molecular weights of PLGA 85:15 at different degradation times for each loading condition were determined using a TOSOH Ambient Temperature GPC (Tetrahydrofuran or THF) with a differential refractive index (RI) detector. The weighted average (M_w) and number average (M_n) molecular weights and the polydispersity index (PDI) were calculated from the GPC data using a series of polystyrene standards. The M_w range of the instrument was 500-1,000,000 g/mol.

3. Results

3.1. Physical Changes.

Figures S1 and 3 show the physical changes of samples under mechanical static loading (7.5 kPa) and immersion in PBS at 37ºC. All the mechanically-loaded samples changed from being transparent to a white opaque color, with significant elongation and a corresponding thinning within the first ten days of being subjected to the loading. The initial transparent color **(**Reference sample at the bottom left of **Figure 3)** before degradation indicated the amorphous nature of the samples. The transformation to a white, opaque color suggested an increase in crystallinity **(Figure S1)**. This phenomenon typically occurs because the

folded chains packed in lamellae of crystalline polymers reflect light, whereas light tends to pass through the random entanglements of chains of amorphous polymer structure[38]. The samples showed extreme creep and reached their maximum potential extension, i.e., reached the bottom of the container, within 10 days of degradation. This elongation is extreme **(Figure S1)**, as the 5 mm portion of the exposed area extended to 220 mm, which represents a 4300% elongation! It was also observed that the samples initially did not exhibit much deformation for a significant amount of time (around 8 days) but that the elongation and thinning were rather quick once the creep began. Indeed, **Figure 3** shows how rapidly, typically within 24 hours, the samples reached the bottom of the container with a travel space of 240 mm. The samples continued slacking due to their own weight and there was no effective loading applied once they reached the bottom of the container. The samples continued to get flaky and more brittle with increasing time, causing difficulty in retrieving them. By day 60, the already paper-thin samples formed a soft inner core with a shell-like outer covering. By day 70, only the outer shell remained. For comparative purposes, we also studied samples immersed in PBS at 37ºC that were not subjected to any mechanical loading. These samples **(Figure S2** also changed to an opaque white color on the surface during immersion, but when cutting through the cross-section of the samples, we observed that the inner core remained transparent until day 20. Unlike their mechanically loaded counterparts, there were no significant changes in the dimensions of the samples by day 10 or 20 of degradation. By day 30, the core turned white and was soft. By days 40-50, the samples greatly swelled and consisted of a liquid core with a solid exterior **(Figure 4A)**. By day 60, the samples slightly elongated due to their own increased weight; cracks formed on the surface of the samples, and some of the liquid trapped inside the core drained into the PBS solution **(Figure 4B)**. By day 70, only a thin shell remained **(Figure 4C)**.

By comparison, no major changes in color were observed in control samples not immersed in PBS (both in samples without mechanical loading and in those subjected to effective stress of 7.5 kPa) but exposed to ambient temperature of 37ºC for 90 days, although the samples slightly lost some transparency as the number of days increased **(Figure S3B)**. This result indicates that PLGA experiences slight aging due to long-term thermal exposure. In the non-loaded samples without PBS, slight shrinkage and widening **(Figure 7A)** were observed. Some of these non-loaded and non-immersed samples also curled **(Figure S3B)**. However, unlike the loaded samples in PBS, the loaded samples without PBS exhibited neither significant changes in dimensions nor any curling **(Figure S3C)**. This indicates that the extreme elongation in the loaded, hydrolyzed samples is a consequence of the combined loading, fluid sorption, hydrolysis, and thermolysis at 37°C. Combined fluid sorption and thermolysis at 37°C does not cause extreme deformation or creep even after 90 days of degradation.

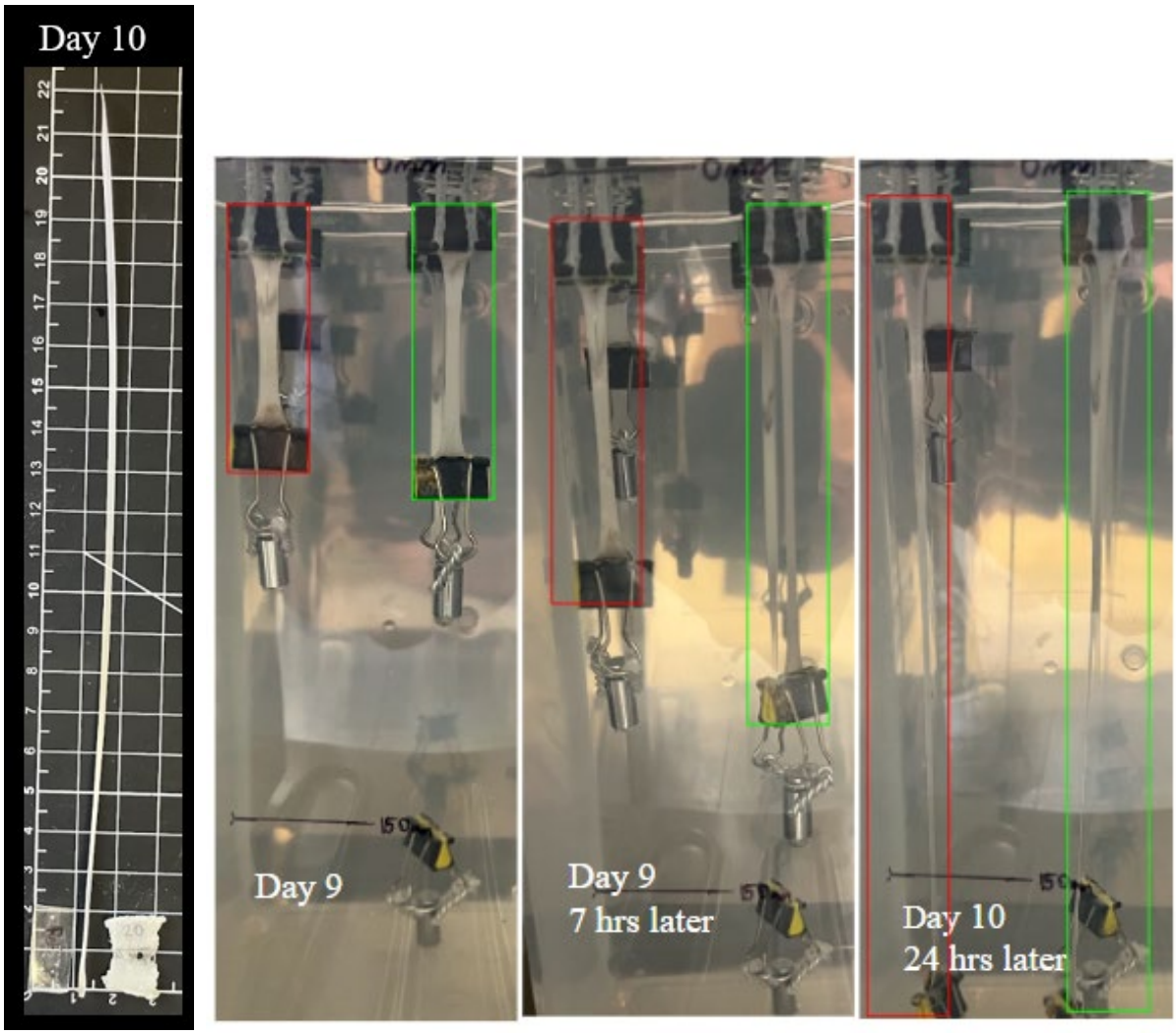

Figure 3. *The first picture shows the effects of mechanical static loading of 7.5 kPa on samples immersed at 37ºC on day 10. The image presents elongated and degraded samples (initially 5 mm exposed length) alongside the degraded gripping portion (8 mm ×2) and a 21 mm (8 mm+5 mm+ 8 mm) reference non-degraded sample before immersion. All values on the scale in the photographs are in cm. The following photographs demonstrate the changes in samples under static mechanical loading observed over a period of 24 hours until day 10 of degradation. After an initially slow elongation, the samples exhibited rapid elongation after the onset of creep.*

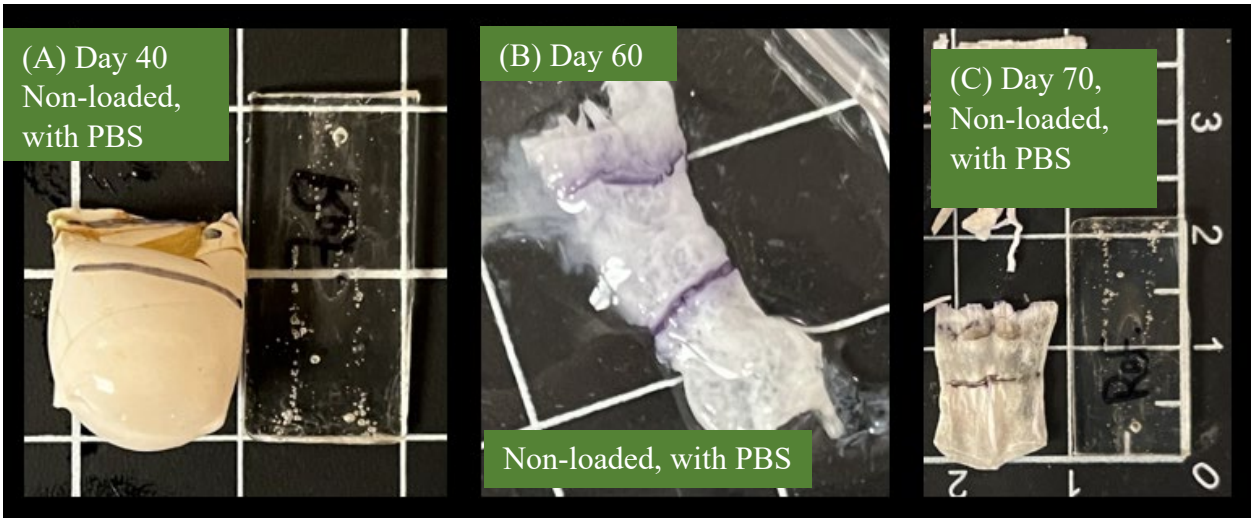

Figure 4. *Samples under no load immersed in PBS at 37°C: (A) non-loaded samples exhibited swelling by day 40; (B) non-loaded samples ruptured with a corresponding loss of the liquid inner core by day 60; (C) only the outer shell remains on day 70 in the non-loaded samples.*

3.2. Mass Loss. Significant mass loss **(Table S1)** was observed in the loaded samples after day 10 and the non-loaded samples after day 20 of degradation **(Figure 5, S4-S6)**. While the loaded samples initially lost mass more rapidly, after day 40, the mass loss of non-loaded samples accelerated, and thereafter the overall mass of the non-loaded samples **(Figure 5)** was much lower than that of the loaded samples. The non-loaded, hydrolyzed samples formed a liquid core by day 40 and were very fragile by day 50. As a result, the liquid core seeped out of the samples, causing a sudden increase in % mass loss in the non-loaded, hydrolyzed samples. In the loaded, hydrolyzed samples, we observe a sudden increase in % mass loss at around day 60 of degradation during which a soft core forms inside the elongated sample. The lower dry weight and higher wet weight of samples under mechanical loading **(Figure 5, S4, S6)** at day 60 compared to day 70 can be attributed to the formation of a soft core on day 60, which, upon drying, stuck to the surface of the container and was more difficult to retrieve. The shell-like structure on day 70 was easier to retrieve from the solution and quantify. The mass loss calculated was defined as

$$\text{Mass loss (\%)} = \frac{m_0 - m}{m_0} \times 100\% \quad (1)$$

Here, m_0 is the initial mass before immersion, and m is the mass after immersion (in the dried condition) on a particular degradation day.

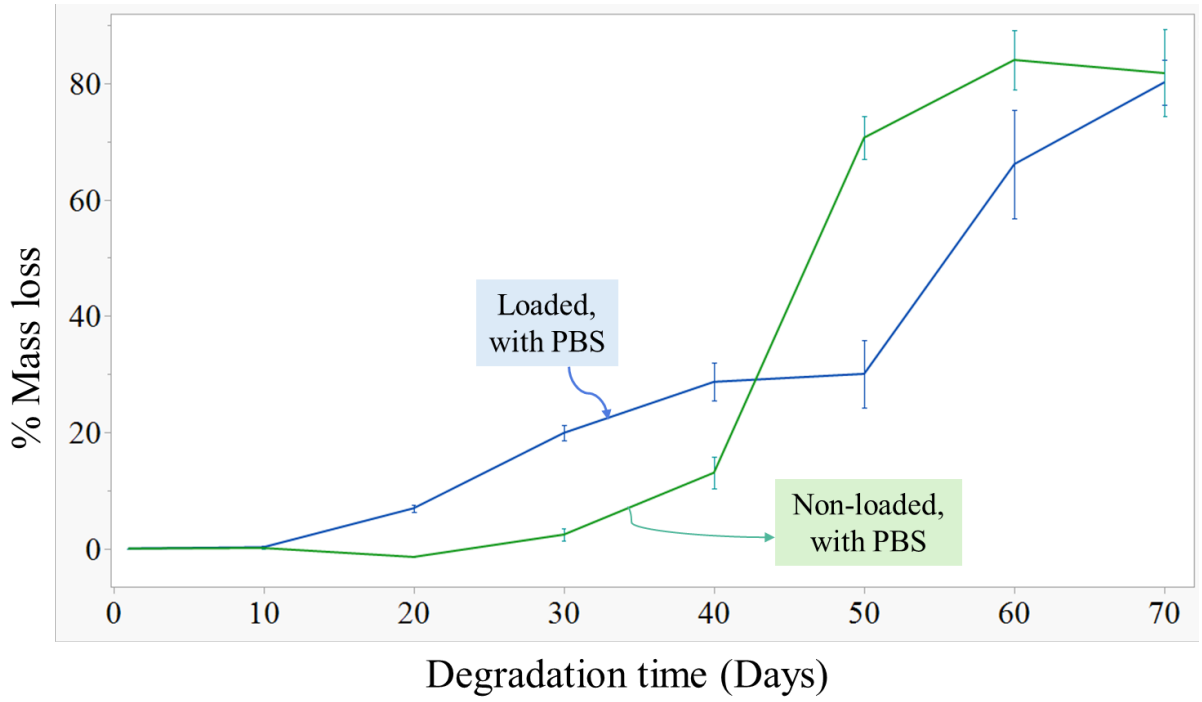

Figure 5. *Mass loss for samples (in dried condition) immersed in PBS at 37ºC, comparing samples subjected to mechanical loading with those not subjected to mechanical loading.*

3.3. Gel Permeation Chromatography. The weight-average (M_w) and number-average (M_n) molecular weight, degree of polymerization (X_n), and polydispersity index (PDI) were obtained from GPC. Four cases were considered to check how PLGA degrades under different conditions. The degree of polymerization **(Table S4)** was calculated using **Equation 3**, where the M_n was divided by the molecular weight of the PLGA copolymer's monomeric weight, considering an 85% contribution from the lactide unit and a 15% contribution from the glycolide unit and a molar mass of 90.08 g/mol and 76.05 g/mol for the lactide and glycolide units, respectively. We note that this formula might not be strictly valid for PLGA after it starts degrading because lactide and glycolide units degrade at different rates. As such, at any given degradation time point, the ratio of lactide and glycolide units might not be the same as before degradation. For the sake of simplicity, the ratio is considered constant for the calculation of X_n in this manuscript.

$$X_n = \frac{M_n}{\left(\frac{85}{100}\right)(90.08\ \text{g/mol}) + \left(\frac{15}{100}\right)(76.05\ \text{g/mol})} = \frac{M_n}{87.99\,\text{g/mol}} \tag{2}$$

Figure 6 (Table S5) shows the time evolution of the number average molecular weight for samples immersed in PBS at 37°C and under no mechanical load. The M_n of the injection-molded samples before they were subjected to hydrolysis, temperature, or immersion (i.e., 0 days) was 34,860 g/mol. The M_n decreased significantly until day 40. Of note, between days 30-40, there was a sudden sharp decrease in M_n. This event coincided with the swelling and formation of an acidic core within the sample. From day 40-70, a bimodal molar mass distribution was observed, indicating the presence of disparate compositions/phases

and inhomogeneous degradation throughout the sample, i.e., corresponding to a solid outer shell and an acidic liquid inner core. The degree of polymerization (X_n) value also demonstrated the formation of oligomers between days 30 and 40 in the PBS-immersed, non-loaded samples, likely indicating the onset of bulk erosion. The outer layer seemed to have a much higher molecular weight compared to the inner core. The overall M_n was skewed towards the M_n of the inner core, which shows that the composition was predominantly highly degraded oligomeric units within the core of the samples with distinct traces of a slowly degrading thin surface. By day 50, this gap seemed to narrow with a significant drop in the M_n of the solid shell on the surface, while not much change in M_n was observed for the inner core. On days 60 and 70, the two components were indistinguishable from one another and had a M_n of 3052 g/mol and 1695 g/mol, respectively, which approached the detection limit of the GPC machine.

Figure 6 (Table S4) also shows the time evolution of the number average molecular weight for samples immersed in PBS at 37°C that were mechanically loaded. The M_n for both loaded (in PBS) and non-loaded (in PBS) samples appeared to follow a surprisingly similar trend until day 30 of degradation, almost overlapping with each other despite being significantly different morphologically and exhibiting very different trends in T_g's. By contrast, the overall M_n was comparatively much lower in the case of no loading (in PBS) after day 30 due to the retention of acidic byproducts within the polymer core, leading to an increase in autocatalysis. The degradation of the loaded (in PBS) samples was much slower due to the lack of retention of acidic byproducts, which slowed down the rate of autocatalysis. While surface and bulk erosion might occur simultaneously in both the loaded and non-loaded, hydrolyzed samples, one of the phenomena might have been overpowering in each case. The degradation of loaded, hydrolyzed samples might have been primarily governed by surface erosion, while the degradation of non-loaded, hydrolyzed samples might have been primarily governed by bulk erosion. The reasons and mechanisms have further been elaborated in **Section 4.2 and 4.3**.

Figure 6 (Table S6) further shows the differences in M_n between the samples immersed in PBS at 37ºC and the samples exposed to 37ºC but not immersed in PBS. The samples undergoing hydrolysis without any external load underwent maximum degradation. In general, both the cases of loaded and non-loaded samples immersed in PBS underwent more degradation compared to the cases of control samples (loaded and non-loaded samples not immersed in PBS). In the control samples, the mechanically loaded samples had lower M_n than the non-loaded samples.

Table S8 and Figure S4 show the polydispersity index (PDI) of the samples under immersion. The PDIs were between 1.7 and 1.8 until day 30 and day 50 for non-loaded and loaded samples under immersion, respectively. After day 30 of degradation for the non-loaded (in PBS) samples, the observed PDI was large due to the bimodal distribution of the molar mass, which can be attributed to the spatially heterogeneous degradation, i.e., with a solid outer layer and a soft and liquid core. We note that the day 50 PDI for non-loaded (in PBS samples), was slightly lower because of the loss of most of the liquid inner core due to its oozing out of the sample. A similar trend can be seen for the loaded samples (in PBS) after day 50 of degradation for a similar reason.

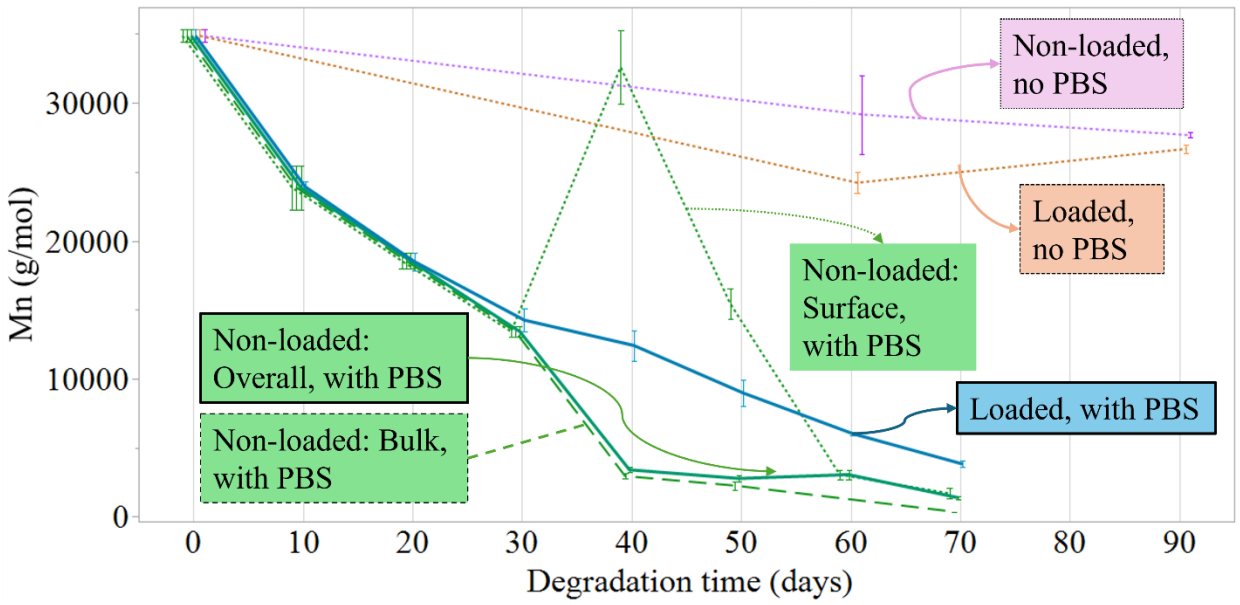

Figure 6. *Comparison of the time evolution of the number average molecular weight among PBS-immersed and mechanically loaded, PBS-immersed and non-loaded, and non-PBS-immersed (loaded and non-loaded) samples at 37ºC.*

3.4. Glass Transition Temperature. **Figure 7** shows the effect of static mechanical loading of 7.5 kPa on the glass transition temperature (T_g) of the samples during immersion in PBS at 37ºC. A steady rise in T_g is observed until day 30: T_g increases from 36.8±0.5ºC on day 0 (before immersion) to 42.5±1.7ºC on day 30 of degradation. This period is followed by a constant decrease in T_g to 38.8±2.4ºC on day 50. By day 60, the samples formed a soft-inner core with a shell-like exterior, resulting in two distinct regions with different glass transition temperatures **(Figure S8)** of 26.2±0.9ºC for the inner core and 43.7±0.6ºC for the outer shell. On day 70, we could only retrieve the outer shell, whose T_g dropped to 40.6±1.0 ºC. It was also observed that overall, the T_g of loaded, hydrolyzed samples was consistently high throughout the degradation process, where even on day 70 of degradation, the T_g was 40.6 ± 1.0 ºC compared to 36.8±0.5ºC before immersion. This observation was interesting because T_g generally tends to decrease with a decrease in M_n.

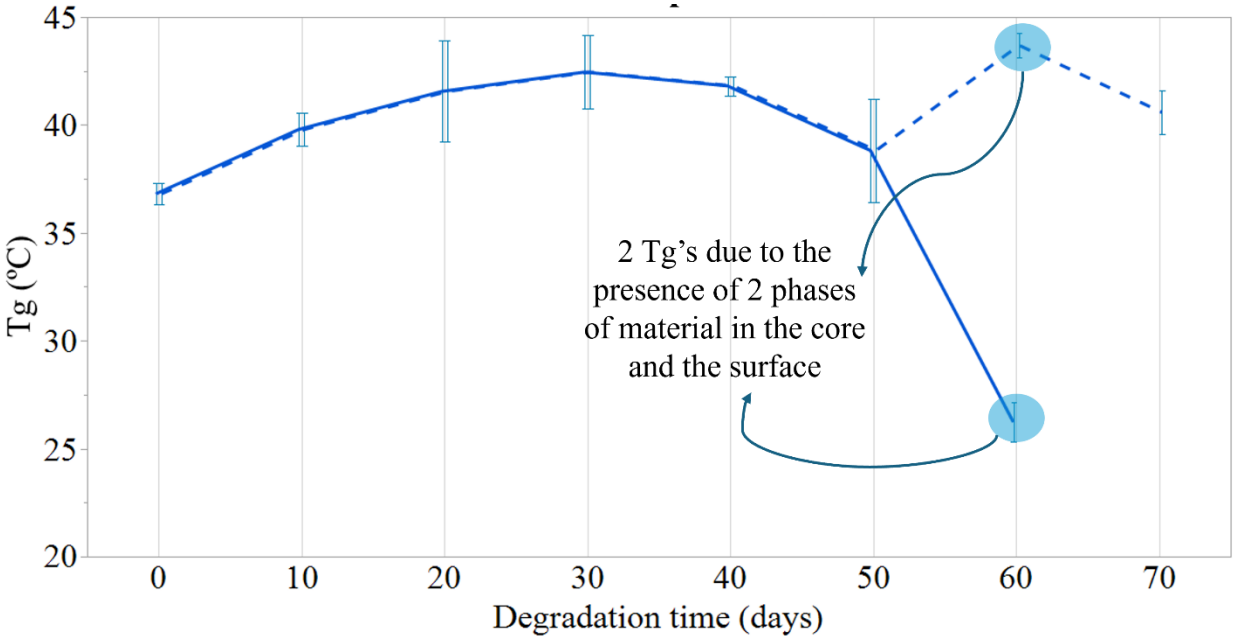

***Figure** 7. The time evolution of the glass transition temperature for samples immersed in PBS at 37ºC under static mechanical load of 7.5 kPa.*

Figure 8 (Table S2) compares the time evolution of glass transition temperature among all samples. The glass transition temperature of the injection-molded samples before they were subjected to hydrolysis, temperature, or the immersion process (i.e., 0 days) was 36.8±0.5ºC. In the samples immersed in PBS without any mechanical loading, an initial slight increase in T_g to 38.4±0.5ºC was observed on day 10. A decrease in T_g then followed until day 30, where the T_g dropped to 29.3±0.7ºC. Two T_g's were observed from day 40 to 70. On day 40, the two observed T_g's were 25.2±0.9 ºC and -17.1±1.2 ºC, indicating two separate states of polymer, due to the formation of an outer solid layer and an inner acidic liquid, respectively. By day 60, the outer layer cracked because of self-weight due to degradation byproduct retention, and the inner liquid with degradation byproducts oozed out of the sample, leaving a very thin shell. The sample was difficult to retrieve without breaking it and losing the inner liquid component. Thus, only the T_g of the outer shell was detected, and observations for the inner portion were not obtained. Between days 40 and 50, the T_g of the inner portion continuously decreased, while the T_g of the outer layer increased. By day 70, the T_g of the thin outer layer decreased again. **Table S2** shows the effect of static mechanical load and no load on the glass transition temperature at each degradation time point for samples immersed in PBS at 37ºC.

Figure 8 (Table S6) also compares the time evolution of T_g of the loaded and non-loaded PBS-immersed samples with the loaded and non-loaded non-immersed control samples. We observed that the glass transition temperatures were lower overall in the case of non-loaded, PBS-immersed samples compared to the loaded, PBS-immersed samples. The inner core exhibited significantly lower T_g compared to any other cases. The trends in T_g in the case of loaded and non-loaded, hydrolyzed samples can be explained as an effect of the combination of changes in composition of the copolymer, crystallinity, water uptake, and the

difference in the retention of degradation products in each case. These reasons and mechanisms are elaborated further in the discussion section. Samples for both the control cases (no PBS-immersion but exposed to 37ºC) exhibited nearly identical trends to each other with a slight overall increase in T_g over time.

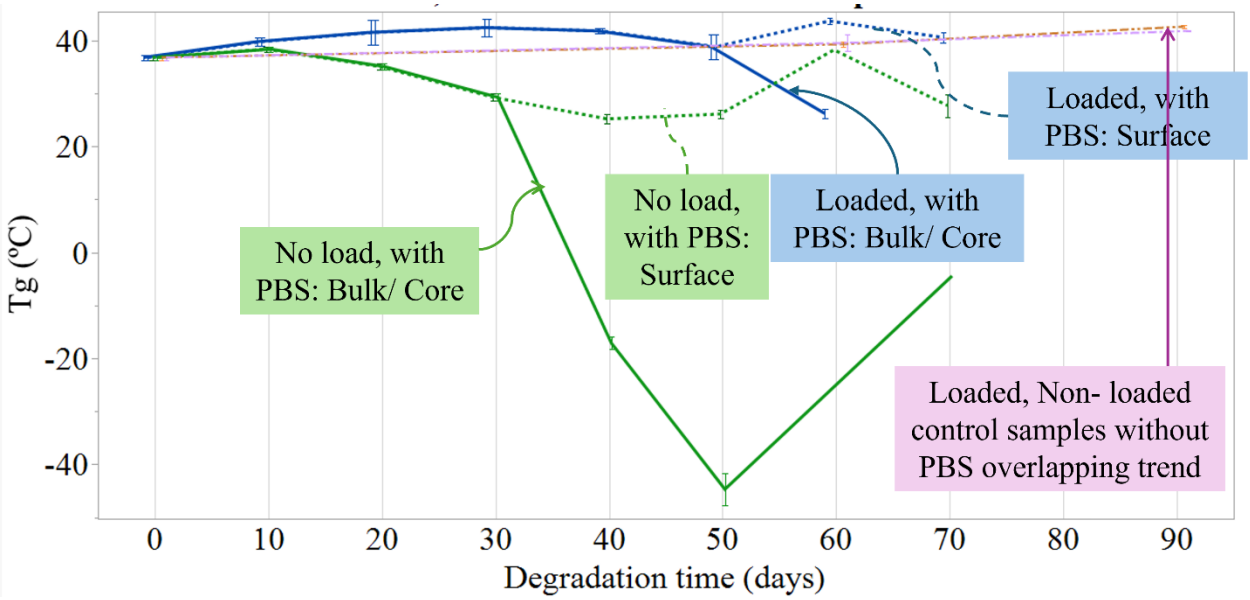

Figure 8. Comparison of the time evolution of the glass transition for PBS-immersed and mechanically loaded, PBS-immersed and non-loaded, and non-PBS-immersed (loaded and non-loaded) samples at 37ºC.

3.5. Crystallinity. For the given DSC parameters, only a melting endotherm was observed, and no cold crystallization peak was observed. Thus, the percent crystallinity was calculated by dividing the area under the melt endotherm (ΔH_m) by the energy required to melt 100% crystalline poly-L-lactide **(Equation 2)**.

$$\%crystallinity = \frac{\Delta H_m}{93.1\ \mathrm{J/g}} * 100\% \tag{3}$$

Since PLGA is a copolymer, there is a lack of data for the reference heat of fusion. Although PGA is more crystalline than PLA [39], the ratio of lactide units in the PLGA specimen used here is much higher. Hence, the heat of fusion of 100% crystalline PLA (i.e., 93.1 J/g[40]) is used. This approach has been taken by previous calculations of the crystallinity of PLGA of similar composition[18, 41, 42]. From this equation, we can deduce that the percent crystallinity is directly proportional to ΔH_m. **Table S3 and Figure 9** show the melt enthalpy and percent crystallinity of samples immersed in PBS at 37°C and subjected to static mechanical loading and no loading. No melt endotherm was observed for non-loaded samples immersed in PBS after day 40. Overall, we observed that the %crystallinity of non-loaded, hydrolyzed samples is higher than that of the loaded, hydrolyzed samples. This observation may stem from the plasticizing effect of water and degradation products retained in the core of non-loaded, hydrolyzed samples and the corresponding

absence thereof in the loaded, hydrolyzed samples. These items are further elaborated in the discussion section.

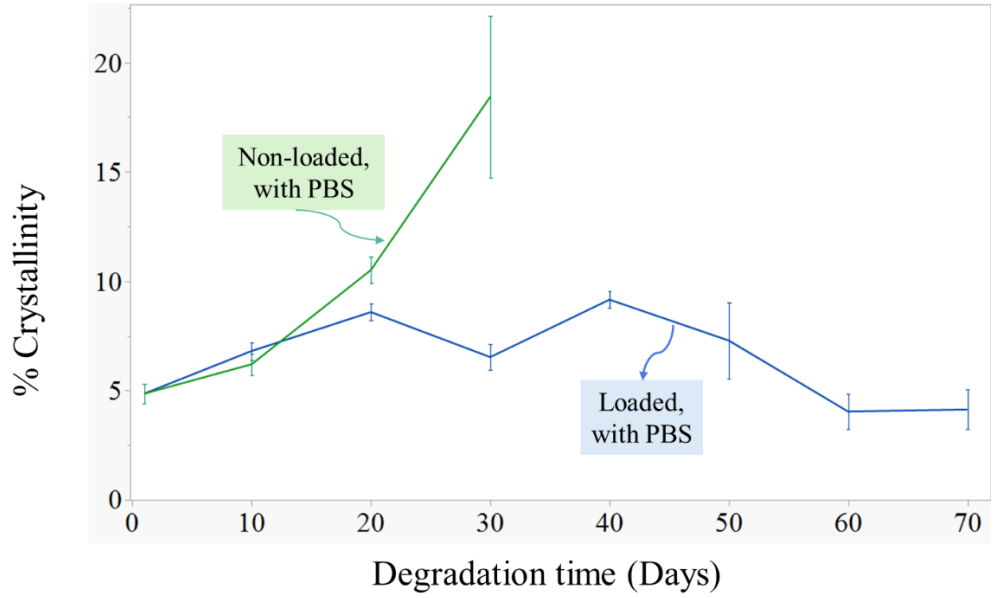

Figure 9. *Comparison of the time evolution of the % crystallinity for PBS-immersed and mechanically loaded, PBS-immersed samples at 37°C.*

4. Discussion

4.1. Key Observations

This study provides insight into the hydrolytic degradation kinetics of PLGA as well as how mechanical loading affects hydrolytic degradation and erosion. Hydrolytic degradation is described as the process of chain scission or the cleavage of the ester bonds from hydrolytic reactions to form oligomers and, consequently, to form monomers[43]. By comparison, erosion is described as an effect of degradation causing a loss of mass into the surrounding media through the diffusion or solubility of the formed oligomers and monomers[44]. Biodegradation of polymers is primarily indicated by molecular changes due to chain scission (degradation) and structural and mass loss due to the loss of the degraded chains into the surrounding media (erosion)[45]. There are two identified modes of erosion: surface and bulk erosion.

Surface erosion is considered a solubility-controlled process, where the resultant products of degradation, i.e., the oligomers and monomers, are readily soluble in the surrounding media. In contrast, bulk erosion is considered as a diffusion-controlled process, where these resultant oligomers and monomers are trapped inside the polymer matrix and escape slowly through a diffusion process[46]. The time evolution of mass, molecular weight, and physical properties of the degrading polymers is correlated with solubility- or diffusion-controlled processes. These details control the rate of degradation and structural stability of the polymer matrix.

In this study, we observed extreme mechanical deformation (4300% elongation and considerable thinning) within just 10 days of PBS immersion in the loaded samples immersed in PBS at 37ºC. The elongation is surprising because the applied stress of 7.5 kPa is extremely small compared to the 20 MPa yield stress of the material at 37ºC. However, no such elongation was observed in samples that were under the same load and temperature but not immersed in PBS. Thus, this drastic elongation in the loaded samples immersed in PBS cannot be simply attributed to the load alone or to the polymer's T_g being between 36.8ºC (before immersion) to 38.4ºC (day 10 of degradation), which is very close to the temperature (37ºC) that the polymer was exposed to during degradation. We also noted that in control samples (no PBS immersion) that were mechanically loaded at 37ºC, we did not observe any elongation. This observation shows that the extreme elongation resulted from the combined effect of loading and hydrolysis. In non-loaded samples, biodegradation leads to the formation of two-phase constituents that differ significantly in their chemical, physical, and mechanical properties (heterogeneous degradation). While one might intuit that such severe elongation observed in the hydrolyzed and mechanically-loaded specimens would induce faster degradation, we instead observed that these specimens degraded much slower than the non-loaded (but hydrolyzed) samples. Additionally, a decrease in the glass transition temperature of a polymer is typically accompanied by a decrease in molecular weight, but herein we observed an increase in T_g with a drop in M_n during the first few weeks of degradation of the loaded samples immersed in PBS. However, despite observing considerable differences in T_g data in the PBS-immersed loaded and non-loaded samples, the M_n measurements herein coincided in both cases until day 30. Also, crystallinity data show that the % crystallinity increases until day 30 for both loaded and non-loaded, hydrolyzed samples. While the effects of crystallinity are not always straightforward, generally, T_g tends to increase with an increase in the % of crystalline regions in a polymer[47].

At first glance, these results might seem counterintuitive due to the significant physical differences in the loaded and non-loaded samples in PBS; the T_g might be affected by three major factors:

1) Change in chemical composition of the copolymer.
2) Retention of acidic byproducts in the non-loaded, hydrolyzed samples and the lack of retention of these byproducts in the loaded, hydrolyzed samples.
3) Differences in water uptake within the polymer matrix.

As such, our results warrant further analysis of the chemistry of PLGA degradation and correlation of all our collected evidence.

4.2. Chemistry of PLGA Degradation

Digging down on this point, it is known that PLGA degrades via hydrolytic cleavage of ester linkages, forming lactide and glycolide units. The carboxylic acidic end group in the lactide unit neutralizes in the PBS, which tends to decrease the autocatalytic reaction rate[48]. By contrast, the glycolide units degrade via cleavage of ester bonds, which increases the acidic microclimate due to the formation of acidic oligomers and tends to increase the autocatalytic reaction rate[49]. Like other aliphatic polyesters, the lactide units have hydrolytically unstable ester linkages in the polymer's backbone. This linkage degrades

through hydrolysis, which is ultimately metabolized to water and carbon dioxide and removed from the body[50]. The lactide units can exist in two optically isomeric forms, semi-crystalline poly-L-lactide (PLA) and amorphous poly-D-lactide (PDLA), due to the presence of a methyl group that causes asymmetry[51]. This methyl group also contributes to the hydrophobicity of lactide units, known as the steric shielding effect, which makes it more resistant to hydrolysis compared to the glycolide units[52]. Both the lactide[53] and glycolide[54] units undergo heterogeneous degradation with surface-center differentiation (i.e., different processes/effects near the center of the specimen as compared to the exterior surface of the specimen). All these reactions happen simultaneously, but the rate of neutralization of the carboxylic group in the lactide unit and the rate of cleavage of the glycolide units might differ based on the composition of the copolymer and external factors including mechanical loading. Effectively, the presence of methyl groups in lactide units makes the polymer more hydrophobic, limiting the water uptake, and the presence of the carboxylic acid end groups decreases the autocatalytic reaction rate. Thus, we can conclude that the higher the percentage of lactide units, the slower the degradation will be. **Figures 10 and 11** schematically display the underlying chemical mechanisms contributing to the degradation and erosion kinetics.

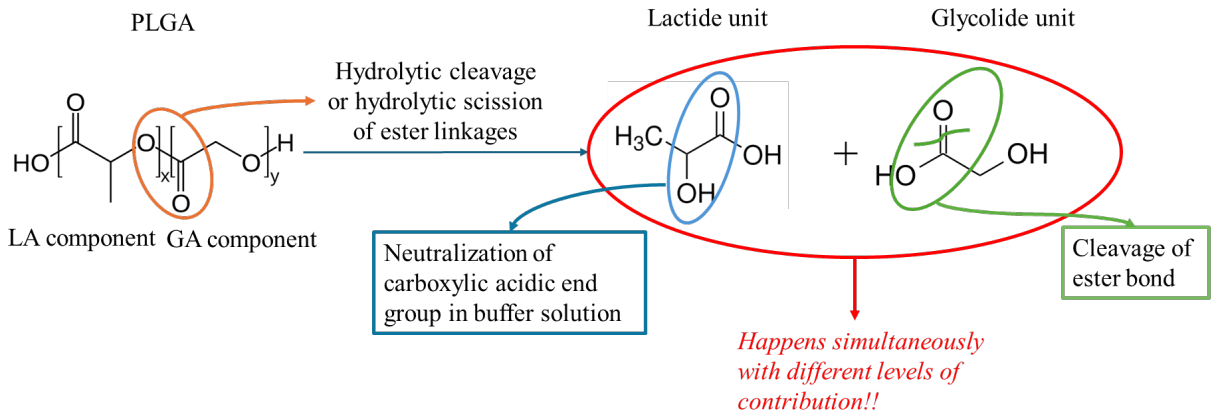

Figure 10. *PLGA undergoes chain scission to form constituent lactide and glycolide units, which further degrade through different chemical mechanisms to release oligomers and monomers.*

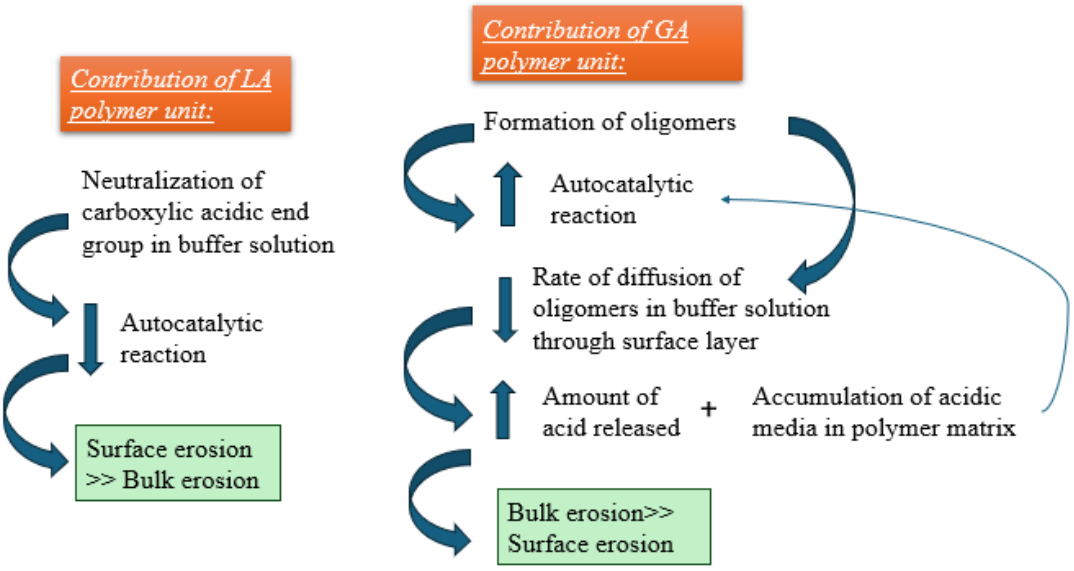

Figure 11. *Contribution of each copolymer unit to the degradation and erosion kinetics.*

4.3. Analysis of the Results

4.3.1. Thermal Analysis and Molecular Degradation

Digging down into the effect of crystallinity, generally in polymers an increase in T_g is expected to correlate with increase in % crystallinity because crystalline regions tend to restrict the movement of the amorphous regions of the polymer. However, this generality does not always hold true in the case of PLGA[47, 55-58]. By contrast, it has been observed in various studies of PLGA that the % crystallinity increases with a decrease in T_g during hydrolysis[59]. This phenomenon occurs because PLGA initiates degradation primarily in the amorphous regions[60]. As such, the degradation in the amorphous region is faster than the crystalline region, leading to a relative increase in the crystalline fraction. The increased mobility of the subsequent broken chains can also lead to the formation of new crystalline structures[61]. Moreover, water sorption and the resultant degradation products during hydrolysis can have a plasticizing effect on the PLGA copolymer that disrupts secondary forces like van der Waals forces and hydrogen bonds within the polymer structure, thereby increasing the free volume, which is reflected as a decrease in T_g[62-64]. The weakening of these intermolecular forces further increases the mobility of the polymer chains, further lowering the T_g. This phenomenon is observed in the non-loaded, hydrolyzed samples, in which we observe an increase in %crystallinity with a decrease in T_g and an overall greater % crystallinity compared to loaded, hydrolyzed samples due to the retention of degradation byproducts and water uptake that contributes to the plasticizing effects on the samples. By contrast, we do not observe this retention of acidic byproducts in the loaded, hydrolyzed samples. Therefore, we observe an increase in % crystallinity with an increase in T_g as the crystalline regions restrict the movement of the amorphous regions in loaded, hydrolyzed samples. However, we observe a dip on day 30, followed by an increase by day 40, and subsequently a decrease until day 70 of degradation in the loaded, hydrolyzed samples. The dip in % crystallinity of loaded, hydrolyzed samples on day 30 may be an artifact due to the sudden change in temperature because of transfer from the incubator (at 37°C) to colder conditions during testing; still, it can be observed that the % crystallinity was

almost similar and consistently high on day 20, 40, and 50. The crystallinity in loaded, hydrolyzed samples significantly decreased only after day 50, which is indeed consistent with the formation of acidic core on day 60 and 70.

Additionally, we also observed that the mass loss in loaded, hydrolyzed samples was higher compared to non-loaded, hydrolyzed samples until day 40. This was due to the easier diffusion of monomers and lesser fluid retention caused by extreme elongation and considerable thinning. Consistently, the crystallinity was also lower in loaded, hydrolyzed samples as fewer monomers were available to promote crystallization due to the enhanced diffusion of monomers into the surrounding media caused by the static loading. Overall, the crystallinity of the non-loaded, hydrolyzed samples was higher due to the plasticizing effects caused by the retention of degradation products and higher water uptake. Whereas the crystallinity of loaded, hydrolyzed samples was lower due to the lower availability of monomers to promote crystallization. While this crystallinity data gives us some insight into the trends in T_g, it does not give us a complete picture.

Now, we will discuss the evidence for a possible change in chemical composition of the PLGA copolymer. With the discussed background information about the chemistry of PLGA hydrolysis in mind, we describe the different biodegradation mechanisms of loaded and non-loaded samples, as depicted **in Figures 12 and 13**. From the data and the physical evidence for the loaded samples, we observed an increase in T_g until day 30, along with a decrease in M_n. The initial uptick in T_g, at least until day 10, can be due to the possible accelerated breaking of polymer chains caused by the external load, which would enhance the diffusion of glycolide units to the surface, consequently leaving behind a higher percentage of lactide units in the polymer structure. Thus, the hypothesized scenario of a higher percentage of lactide units seems to be a plausible explanation, as lactic acid has a higher T_g; as such, the higher the concentration of lactic acid, the higher the T_g of the polymer. It could also be attributed to a combination of both changes in crystallinity and faster depletion of glycolide units compared to lactide units. In literature, this phenomenon is usually observed at the end of degradation, where only lactide units are left that degrade very slowly, as observed by Vey[65]. This hypothesis is further fortified by the mass loss data, which shows a mass loss of 7.9% by day 20 and 20.4% by day 30 in the mechanically loaded (in PBS) samples, which can be compared to the non-loaded (in PBS) samples, which exhibit water uptake until day 20 and a mass loss of just 3.0% by day 30. Also, a higher lactide unit concentration engenders a decreased autocatalytic reaction rate, which is generally conducive to surface erosion, which explains the slower degradation rate in the loaded PBS-immersed samples and further substantiates our hypothesis of higher lactide unit concentration therein. On days 40 and 50, we observed a decrease in T_g, M_n, and mass for the loaded PBS-immersed samples, which might indicate that the lactide units also started to degrade along with the glycolide units, albeit at a slow rate. On day 60 in these loaded PBS-immersed samples, we observed slight puffing with a distinct outer shell and an inner soft core **(Figure 4)**, which resulted in two apparent T_g's as well as a decrease in M_n. Only an outer shell is left by day 70 in these samples, with a further decrease in T_g and M_n. While a decrease in molecular weight is usually associated with hydrolytic degradation, mass loss is a physical quantity and directly associated with the erosion process. Steady mass loss is often an indicator of surface erosion, and abrupt mass loss is often an indicator of bulk erosion. From **Figures S4-6**, we can see that the mass loss (dry weight) in the mechanically-loaded PBS-immersed samples was comparatively steady, which again suggests surface erosion at least until day 50 of degradation.

On carefully examining our data and the corresponding physical observations for the samples that were not mechanically loaded during immersion in PBS, we see an initial slight increase in T_g, which can be attributed to an increase in the percent crystallinity of the sample. Next, we see a gradual decrease in T_g until day 30, accompanied by a decrease in molecular weight and slight mass loss. The formation of a liquid core by day 40; the coinciding sharp decrease in molecular weight by day 40; and an abrupt mass loss

around this time all suggest bulk erosion. The observation of two distinct T_g's and two distinct M_n's after day 30 indicate a heterogeneous composition, the outer layer consisting of primarily lactide units contributing to the higher T_g and the inner core comprised of primarily glycolide units with lower T_g that quickly break down into acidic oligomers and monomers which eat the sample from within, accelerating the degradation from the autocatalytic process.

Although not nearly as prominent as in the samples immersed in PBS, a decrease in molecular weight was also seen in both cases of the control samples (i.e., the samples that were kept at 37°C but not immersed in PBS). This decrease can be attributed to the polymer's physical ageing at 37°C. Physical ageing tends to increase the polymer's overall crystallinity, while chemical ageing is responsible for the breakage of molecular bonds, causing chain scission and an eventual decrease in crystallinity. **Table S7** shows a clear increase in crystallinity in the control samples over time (i.e., in both the loaded and non-loaded samples not immersed in PBS).

In comparing our work to the existing body of literature, Dreher[21] performed a study assessing mechanical effects on hydrolytic degradation of PLGA samples and obtained two data points at 6 and 12 weeks. Although limited in its findings, their work concluded that the changes in degradation kinetics stemming from mechanical loading were not associated with the changes in polymer crystallinity, which aligns with our results. While they also noticed an effect of delayed molecular weight loss with the degradation in the loaded specimens, they stated it as a cause without correlating it with the T_g data. Instead, they present these changes in molecular weights as mere consequences of the chemical reactions going on within the sample facilitated by external factors, including mechanical loading. Moreover, the levels of creep deformation observed in their study was significantly limited compared to our observations, which may be attributed to a different formulation of PLGA used in their studies as compared to ours. The extreme strain observed in our experiments and the consequent thinning of the samples can have a serious effect on the erosion process, which may not have been accounted for in the previous study. Herein, we have gathered much more detailed information by further probing the degradation process at a 10-day interval until day 70. Moreover, we also hypothesized as to the plausible causes of the trends and behavior of the hydrolytic degradation of PLGA polymer due to loading and no-loading at a chemical structural level.

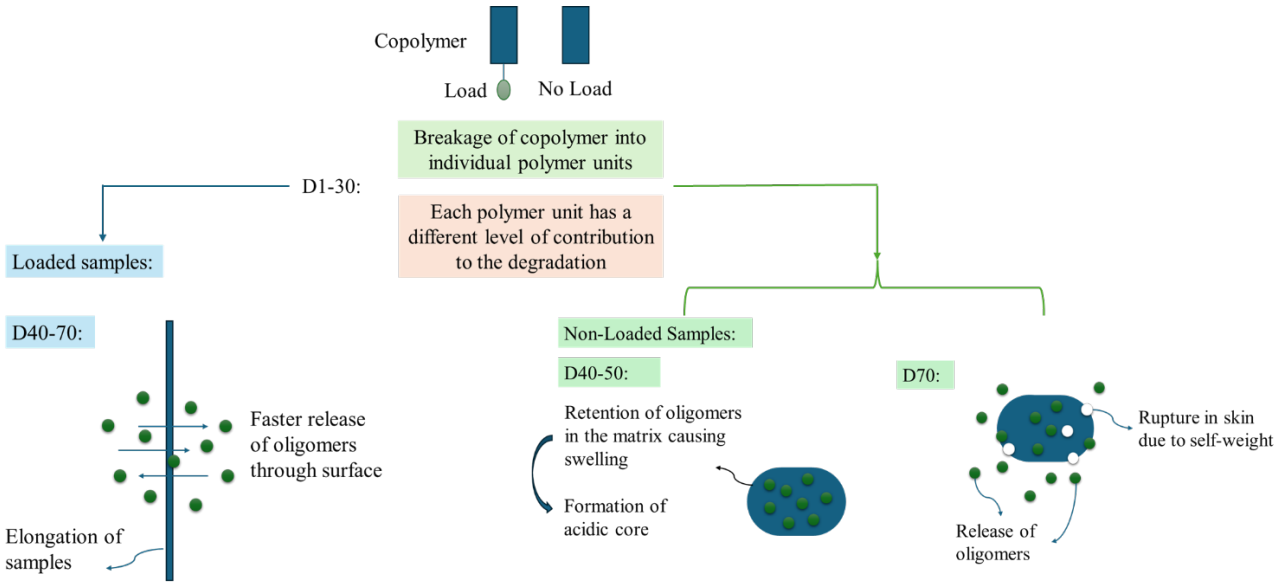

Figure 12. *Comparison of the time evolution of PBS-immersed and mechanically loaded with PBS-immersed and non-loaded PLGA samples at 37ºC.*

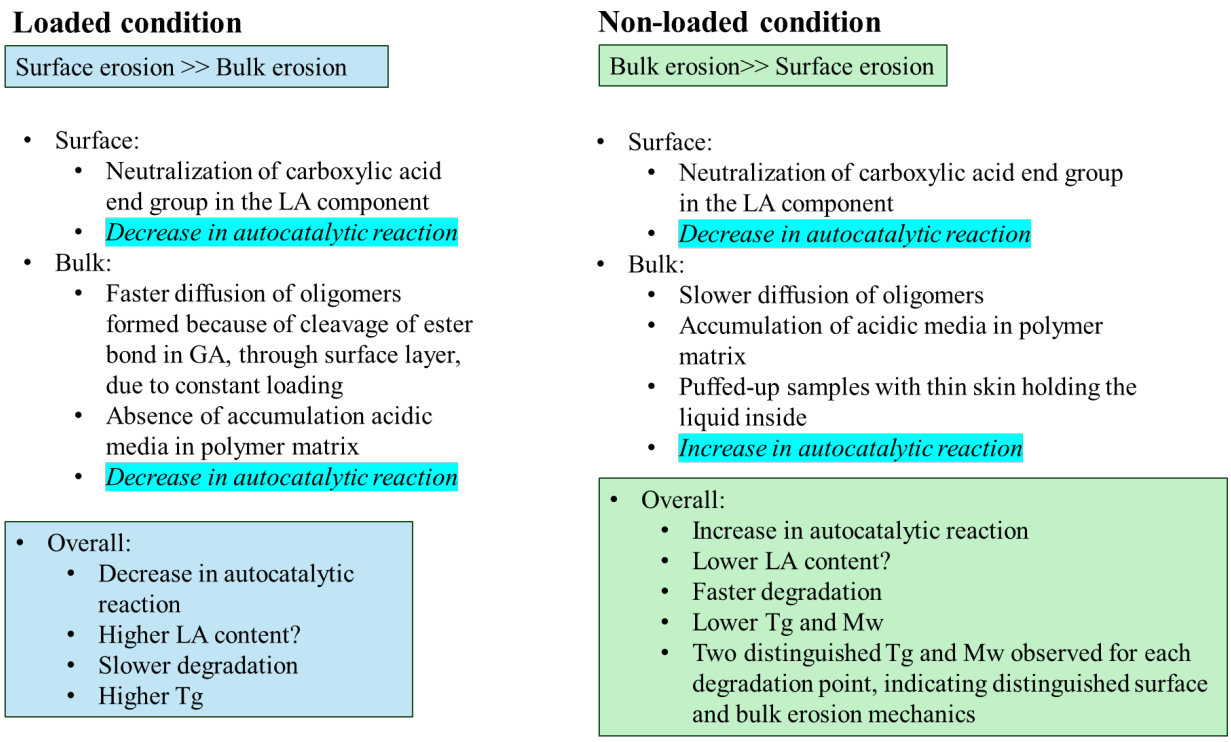

Figure 13. *Highlights of the time evolution of PBS-immersed and mechanically loaded samples at 37ºC where surface erosion is dominant (indicated in the blue box) and PBS-immersed and non-loaded PLGA samples at 37ºC where bulk erosion is dominant (indicated in the green box).*

4.3.2. Physical Changes

Another interesting observation was the suddenness of the elongation of the loaded samples in PBS. The observed 4300% elongation in the loaded samples in PBS occurred between days 9 and 10 of degradation within just 24 hours **(Figure. 3)**. The fabricated PLGA samples were initially relatively stiff before immersion or exposure to 37°C. After immersion at 37°C, the samples became more compliant (they could be easily bent by hand upon slight application of force). This change was followed by a sudden elongation between days 9 and 10 in the loaded, hydrolyzed samples which show that the polymer was ductile until day 10. However, after this elongation of the loaded and hydrolyzed samples, by day 11 the polymer became brittle (the polymer readily crumbles upon touch). This sudden elongation and subsequent embrittlement in the loaded, hydrolyzed samples is likely due to changes in molecular chain mobility, crystallinity, and degradation of the polymers[66].

Indeed, polymer ductility is often attributed to its chain entanglement and mobility. The higher the chain entanglement, the greater its ability to resist localized stress by distributing the force across a larger network, allowing for greater plastic deformation before failure. This process essentially enables the material to stretch and absorb energy rather than breaking easily[67]. Entanglements also limit the movement of

individual polymer chains, allowing them to slide past each other more gradually under stress, thus engendering plastic deformation. We also note that chain entanglement is related to the molecular weight of the polymer. Usually, a higher molecular weight is more conducive to higher chain entanglement. In a related manner, ductile-to-brittle transitions in polymers are associated with a critical molecular weight known as the entanglement molecular weight, M_c, which is the molecular weight at which polymer chains become large enough to entangle[68]. It is a critical value that affects a polymer's physical properties, such as viscosity, ductility, mechanical strength, and adhesion [69, 70]. Below M_c, the chains are unlikely to entangle due to their shorter length, limiting their ability to interweave with other chains. Lower entanglement also leads to relatively low energy absorption capabilities decreasing the polymer's ductility. Also, higher M_w materials have more chain interactions to overcome before polymer chains can begin moving and thus require greater energy and sufficient free volume for rotational motions to proceed, even when chain entanglement occurs.

Entanglement has been seen to begin at a critical polymer molecular weight M_c of 3–4 kDa for PEG melts. For PLGA, the likelihood of entanglement is reportedly poor at M_c below ~7-8 kDa[71, 72], with this value depending on the composition of the copolymer. However, we observe embrittlement in loaded, hydrolyzed samples at around day 11 (between day 10 and 20 according to the M_w measurements). The weight-average molecular weight (M_w) measurements between days 10 and 20 for loaded, hydrolyzed samples were around 41 kDa and 31 kDa **(Table S5),** respectively. However, no embrittlement was observed in non-loaded, hydrolyzed samples by day 10 (M_w: 40 kDa) or day 20 (M_w: 31 kDa) of degradation despite having similar molecular weights as compared to the loaded, hydrolyzed samples **(Table S4)**. Some embrittlement on the surface was observed in the non-loaded, hydrolyzed samples but the core was liquid due to the accumulation of the acidic byproducts in the polymer between day 40 (M_w: 11 kDa) and day 50 (M_w: 3 kDa) of degradation. These observations suggest two key hypotheses: (i) embrittlement can occur at a critical molecular weight (M_c) between 41 kDa and 31 kDa (for loaded, hydrolyzed samples), which is significantly higher than the previously reported M_c of 7-8 kDa for PLGA[71, 72]; and (ii) in the non-loaded, hydrolyzed samples, embrittlement is observed on the surface between day 40 and 50 with M_w between 11 kDa and 3 kDa, respectively, which is close to the previously reported M_c of 7-8 kDa for PLGA[71, 72]. Together, these observations might indicate that loading affects the entanglement of the polymer, causing embrittlement after day 10 and a shift in entanglement molecular weight (M_c) from the reported 7-8 kDa to observed between 31-41 kDa. This shift in M_c can arise as the polymer chains rearrange and it becomes difficult to entangle due to the presence of load, even if the chains are sufficiently long for entanglement. Chain length is directly associated with molecular weight: a higher chain length corresponds to a higher molecular weight. As per our hypotheses, the samples under load during hydrolysis are unable to entangle at larger chain lengths, resulting in higher M_c because the load causes chain rearrangement and restricts the chain mobility.

Moreover, autocatalysis itself can lower the chain entanglement weight[73, 74]. We observe that the loaded, hydrolyzed samples become significantly thinner, allowing easier diffusion of monomers and the fluid out of the polymer matrix. As a result, the loaded, hydrolyzed samples do not retain the degradation products, and subsequently, the autocatalysis is slowed. However, the non-loaded, hydrolyzed samples retain these degradation products, which contribute to autocatalysis. The reduction in chain length and overall concentration of the polymer due to autocatalysis-induced chain scission can directly influence the entanglement behavior. Shorter chains will have fewer opportunities to entangle with each other, and the entanglement density (the number of entanglements per unit volume) will decrease. Thus, in this case, the higher chain entanglement weight in loaded, hydrolyzed samples is due to the slower autocatalysis reaction due to the absence of acidic core containing the degradation by-products. Still, we note that the exact value

of M_c can be determined from a plot containing the log of melt-viscosity and the log of M_w of the polymer, and the above-mentioned hypotheses thus require further investigation.

Alternatively, this ductile-to-brittle transition in the loaded, hydrolyzed samples after day 10 can also possibly be due to strain hardening effects[75]. The external force might have induced order within the polymer chains while maintaining the degree of crosslinking or entanglement between chains[75, 76].

5. Conclusions

We have found that mechanical loading can greatly affect the hydrolytic degradation of PLGA. Although the mechanically-loaded (in PBS) specimens experienced extreme deformation, they degraded much slower than the specimens that were not subjected to mechanical loading (in PBS). At first glance, the initial molecular weight data (here within the first 30 days of degradation) might give the impression that the degradation of the loaded and non-loaded samples immersed in PBS is initially the same. However, similar data does not necessarily imply that the same underlying mechanisms are at play. Correlating the molecular weight data with the glass transition temperature, crystallinity, mass loss, and physical evidence indeed suggests differences in the underlying causes of this degradation. These underlying causes are the possible change in chemical composition of the copolymer, retention and release of the acidic byproducts, and the resultant degradation and erosion processes.

While both the loaded and non-loaded samples in PBS might have undergone changes in chemical composition of the copolymer, the loaded, hydrolyzed samples might have undergone a premature release of the degraded glycolide units due to the presence of the external load. The degradation was more homogeneous, and this premature release of glycolide units caused an overall increase in % of lactide units which is associated with slower autocatalytic rate concentrated on the surface of the copolymer, higher T_g, and less water uptake due to the hydrophilicity of lactide units. This premature release of acidic byproducts resulted in the lack of formation of an acidic core and a resultant slower degradation rate compared to the non-loaded, hydrolyzed samples. This increase in % of lactide units can also help explain the increase in T_g with a decrease in M_n. Again, the lack of retention of the acidic byproducts and less water uptake resulted in an increase in %crystallinity with an increase in T_g.

The non-loaded samples immersed in PBS retained the acidic byproducts and had higher water uptake, which resulted in faster degradation rates. This phenomenon also resulted in heterogeneous degradation, i.e., the composition of the polymer was not constant through its thickness: the outer layer in the non-loaded (in PBS) samples was a solid and had a higher T_g compared to the inner core, which was a liquid. The inner core degraded faster than the surface. The inner core primarily consisted of the degraded by products, primarily glycolide units that degrade faster and have lower T_g, and the lactide units were concentrated on the surface that have relatively slower degradation rate and higher T_g. Due to the lack of mechanical loading, the degradation products were retained causing an overall increase in autocatalytic effect and faster degradation rate. The retention of degradation products and higher water uptake (due to the presence of relatively higher glycolide units compared to loaded, hydrolyzed samples) have plasticizing effects that increases the %crystallinity while decreasing the T_g. Based on our observations, it can also be concluded that these drastic changes (morphologically or chemically) cannot be simply attributed to either the mechanical loading or the T_g of the material being close to the immersion temperature alone. Unlike the samples subjected to mechanical loading while immersed in PBS, the samples that were mechanically loaded but not immersed in PBS showed little to no change in their morphology, and only slight decreases in T_g and M_n that can be attributed to physical ageing. Overall, we can assert that while mechanical loading certainly influences the degradation kinetics of the polymer. The effects of mechanical loading are significantly amplified when it is combined with fluid sorption and hydrolysis..

Morphologically, we observed extreme elongation (4300%) in samples subjected to mechanical loading (at 37°C in PBS), whereas the samples without any mechanical loading (at 37°C in PBS) exhibited the most significant chemical changes that resulted in the fastest degradation. Connecting our observations to practical applications, i.e, during use in biomedical implants or drug delivery, PLGA is subjected to various mechanical loads and simultaneously undergoes hydrolysis. The manner in which a polymer like PLGA degrades and the consequent mode of degradation can affect the structural stability of the implants and alter the drug release profile. From our observations, we can see how mechanical loading can have a significant impact when combined with hydrolysis. We also note that different compositions of PLGA might yield different results. As such, future studies in this area should target systematic characterization that links specified levels of stress and strain (including compression) and the composition of PLGA to its hydrolytic degradation behavior. Spatial quantification of the lactide and glycolide units throughout the degradation time will also provide a better understanding of the underlying mechanisms. Overall, we hope that our study will help inform practical implementation of PLGA in biomedical implants, bringing us a step closer to guiding designs with precisely tailored degradation behavior.

CRediT authorship contribution statement

Devleena Samanta: Writing- Original Draft, Methodology, Investigation, Data Curation, Formal Analysis, Validation. **John A. Koithan:** Investigation, Data Curation. **Anastasia H. Muliana:** Conceptualization, Funding Acquisition, Project Administration, Methodology, Writing- Review & Editing. **Matt Pharr:** Conceptualization, Funding Acquisition, Project Administration, Methodology, Writing- Review & Editing.

Declaration of competing interest

The authors declare that they have no known competing financial interests or personal relationships that could have appeared to influence the work reported in this paper.

AcknowledgementsThe authors acknowledge the support of the National Science Foundation, United States under award number CMMI-2013696. The authors also acknowledge the characterization part of this work was performed in the Texas A&M University Soft Matter Facility (RRID:SCR_022482).

Figure captions:

Figure 1. *Schematic of PLGA specimens under static mechanical loading of 7.5 kPa, undergoing hydrolytic degradation in-vitro. The specimens are maintained in PBS, and the entire set-up is housed in an incubator at 37ºC and 90% humidity.*

Figure 2. *Schematic of sample grip and exposed area for a loaded sample and non-loaded sample.*

Figure 3. *The first picture shows the effects of mechanical static loading of 7.5 kPa on samples immersed at 37ºC on day 10. The image presents elongated and degraded samples (initially 5 mm exposed length) alongside the degraded gripping portion (8 mm ×2) and a 21 mm (8 mm+5 mm+ 8 mm) reference non-degraded sample before immersion. All values on the scale in the photographs are in cm. The following photographs demonstrate the changes in samples under static mechanical loading observed over a period of 24 hours until day 10 of degradation. After an initially slow elongation, the samples exhibited rapid elongation after the onset of creep.*

Figure 4. *Samples under no load immersed in PBS at 37ºC: (A) non-loaded samples exhibited swelling by day 40; (B) non-loaded samples ruptured with a corresponding loss of the liquid inner core by day 60; (C) only the outer shell remains on day 70 in the non-loaded samples.*

Figure 5. *Mass loss for samples (in dried condition) immersed in PBS at 37ºC, comparing samples subjected to mechanical loading with those not subjected to mechanical loading.*

Figure 6. *Comparison of the time evolution of the number average molecular weight among PBS-immersed and mechanically loaded, PBS-immersed and non-loaded, and non-PBS-immersed (loaded and non-loaded) samples at 37ºC.****Figure 7.*** *The time evolution of the glass transition temperature for samples immersed in PBS at 37ºC under static mechanical load of 7.5 kPa.*

Figure 8. *Comparison of the time evolution of the glass transition for PBS-immersed and mechanically loaded, PBS-immersed and non-loaded, and non-PBS-immersed (loaded and non-loaded) samples at 37ºC.*

Figure 9. *Comparison of the time evolution of the % crystallinity for PBS-immersed and mechanically loaded, PBS-immersed samples at 37ºC.*

Figure 10. *PLGA undergoes chain scission to form constituent lactide and glycolide units, which further degrade through different chemical mechanisms to release oligomers and monomers.*

Figure 11. *Contribution of each copolymer unit to the degradation and erosion kinetics.*

Figure 12. *Comparison of the time evolution of PBS-immersed and mechanically loaded with PBS-immersed and non-loaded PLGA samples at 37ºC.*

Figure 13. *Highlights of the time evolution of PBS-immersed and mechanically loaded samples at 37ºC where surface erosion is dominant (indicated in the blue box) and PBS-immersed and non-loaded PLGA samples at 37ºC where bulk erosion is dominant (indicated in the green box).*

References

1. Pachence, J.M. and J. Kohn, *Biodegradable polymers.* Principles of tissue engineering, 2000. **22**: p. 263-277.
2. Kwon, G. and D. Furgeson, *Biodegradable polymers for drug delivery systems*, in *Biomedical polymers*. 2007, Elsevier. p. 83-110.
3. Pillai, O. and R. Panchagnula, *Polymers in drug delivery.* Current opinion in chemical biology, 2001. **5**(4): p. 447-451.
4. Martina, M. and D.W. Hutmacher, *Biodegradable polymers applied in tissue engineering research: a review.* Polymer International, 2007. **56**(2): p. 145-157.
5. Martins, C., et al., *Functionalizing PLGA and PLGA derivatives for drug delivery and tissue regeneration applications.* Advanced healthcare materials, 2018. **7**(1): p. 1701035.
6. Penning, J., H. Dijkstra, and A. Pennings, *Preparation and properties of absorbable fibres from L-lactide copolymers.* Polymer, 1993. **34**(5): p. 942-951.
7. Gogolewski, S. and A. Pennings, *Resorbable materials of poly (l-lactide). II. Fibers spun from solutions of poly (l-lactide) in good solvents.* Journal of Applied Polymer Science, 1983. **28**(3): p. 1045-1061.
8. Park, S., et al., *Adaptive and multifunctional hydrogel hybrid probes for long-term sensing and modulation of neural activity.* Nature communications, 2021. **12**(1): p. 3435.

9. Moghadasi, K., et al., *A review on biomedical implant materials and the effect of friction stir based techniques on their mechanical and tribological properties.* Journal of Materials Research and Technology, 2022. **17**: p. 1054-1121.
10. Göpferich, A., *Polymer bulk erosion.* Macromolecules, 1997. **30**(9): p. 2598-2604.
11. Göpferich, A., *Mechanisms of polymer degradation and erosion.* The biomaterials: silver jubilee compendium, 1996: p. 117-128.
12. Göpferich, A., D. Karydas, and R. Langer, *Predicting drug release from cylindric polyanhydride matrix discs.* European journal of pharmaceutics and biopharmaceutics, 1995. **41**(2): p. 81-87.
13. Zhong, S., P. Doherty, and D. Williams, *The effect of applied strain on the degradation of absorbable suture in vitro.* Clinical materials, 1993. **14**(3): p. 183-189.
14. Smutz, W., et al., *Mechanical test methodology for environmental exposure testing of biodegradable polymers.* Journal of Applied Biomaterials, 1991. **2**(1): p. 13-22.
15. Miller, N. and D. Williams, *The in vivo and in vitro degradation of poly (glycolic acid) suture material as a function of applied strain.* Biomaterials, 1984. **5**(6): p. 365-368.
16. Klouda, L., et al., *Effect of biomimetic conditions on mechanical and structural integrity of PGA/P4HB and electrospun PCL scaffolds.* Journal of Materials Science: Materials in Medicine, 2008. **19**: p. 1137-1144.
17. Kang, Y., et al., *A study on the in vitro degradation properties of poly (l-lactic acid)/β-tricalcuim phosphate (PLLA/β-TCP) scaffold under dynamic loading.* Medical engineering & physics, 2009. **31**(5): p. 589-594.
18. Dreher, M.L., et al., *Characterization of load dependent creep behavior in medically relevant absorbable polymers.* Journal of the Mechanical Behavior of Biomedical Materials, 2014. **29**: p. 470-479.
19. Smith, A.N., et al., *Characterization of degradation kinetics of additively manufactured PLGA under variable mechanical loading paradigms.* Journal of the Mechanical Behavior of Biomedical Materials, 2024. **153**: p. 106457.
20. Li, P., et al., *Influences of tensile load on in vitro degradation of an electrospun poly (l-lactide-co-glycolide) scaffold.* Acta biomaterialia, 2010. **6**(8): p. 2991-2996.
21. Dreher, M.L., S. Nagaraja, and J. Li, *Creep loading during degradation attenuates mechanical property loss in PLGA.* Journal of Biomedical Materials Research Part B: Applied Biomaterials, 2015. **103**(3): p. 700-708.
22. Agrawal, C.M., et al., *Elevated temperature degradation of a 50: 50 copolymer of PLA-PGA.* Tissue engineering, 1997. **3**(4): p. 345-352.
23. Mitchell, M.K. and D.E. Hirt, *Degradation of PLA fibers at elevated temperature and humidity.* Polymer Engineering & Science, 2015. **55**(7): p. 1652-1660.
24. Arhant, M., M. Le Gall, and P.-Y. Le Gac, *Non-Arrhenian hydrolysis of polyethylene terephthalate–A 5-year long aging study above and below the glass transition temperature.* Polymer Degradation and Stability, 2023. **215**: p. 110439.
25. Grasso, M., et al., *Effect of temperature on the mechanical properties of 3D-printed PLA tensile specimens.* Rapid Prototyping Journal, 2018. **24**(8): p. 1337-1346.
26. Zolnik, B.S., P.E. Leary, and D.J. Burgess, *Elevated temperature accelerated release testing of PLGA microspheres.* Journal of Controlled Release, 2006. **112**(3): p. 293-300.
27. Liu, G. and K. McEnnis, *Glass transition temperature of PLGA particles and the influence on drug delivery applications.* Polymers, 2022. **14**(5): p. 993.
28. Shi, M., et al., *Hydrolysis embrittles poly (lactic acid).* MRS Bulletin, 2023. **48**(1): p. 45-55.
29. Li, Y., et al., *The effect of mechanical loads on the degradation of aliphatic biodegradable polyesters.* Regenerative Biomaterials, 2017. **4**(3): p. 179-190.

30. Guo, M., et al., *The effects of tensile stress on degradation of biodegradable PLGA membranes: A quantitative study.* Polymer Degradation and Stability, 2016. **124**: p. 95-100.
31. Lanao, R.P.F., et al., *Physicochemical properties and applications of poly (lactic-co-glycolic acid) for use in bone regeneration.* Tissue Engineering Part B: Reviews, 2013. **19**(4): p. 380-390.
32. Rocha, C.V., et al., *PLGA-based composites for various biomedical applications.* International journal of molecular sciences, 2022. **23**(4): p. 2034.
33. Su, Y., et al., *PLGA-based biodegradable microspheres in drug delivery: recent advances in research and application.* Drug delivery, 2021. **28**(1): p. 1397-1418.
34. Sun, F., et al., *Application of 3D-printed, PLGA-based scaffolds in bone tissue engineering.* International journal of molecular sciences, 2022. **23**(10): p. 5831.
35. Abbasnezhad, N., et al., *On the importance of physical and mechanical properties of PLGA films during drug release.* Journal of Drug Delivery Science and Technology, 2021. **63**: p. 102446.
36. Abbasnezhad, N., et al., *Development of a model based on physical mechanisms for the explanation of drug release: Application to diclofenac release from polyurethane films.* Polymers, 2021. **13**(8): p. 1230.
37. Abbasnezhad, N., et al., *In vitro study of drug release from various loaded polyurethane samples and subjected to different non-pulsed flow rates.* Journal of Drug Delivery Science and Technology, 2020. **55**: p. 101500.
38. Molnár, J., et al., *Modeling of light scattering and haze in semicrystalline polymers.* Journal of Polymer Science, 2020. **58**(13): p. 1787-1795.
39. Magazzini, L., et al., *The Blending of Poly (glycolic acid) with Polycaprolactone and Poly (l-lactide): Promising Combinations.* Polymers, 2021. **13**(16): p. 2780.
40. O'Connor, A., A. Riga, and J. Turner II, *Determination of crystalline content gradients in cold-drawn poly-L-lactic acid films by DSC.* Journal of thermal analysis and calorimetry, 2004. **76**(2): p. 455-470.
41. Landes, C., A. Ballon, and C. Roth, *In-patient versus in vitro degradation of P (L/DL) LA and PLGA.* Journal of Biomedical Materials Research Part B: Applied Biomaterials: An Official Journal of The Society for Biomaterials, The Japanese Society for Biomaterials, and The Australian Society for Biomaterials and the Korean Society for Biomaterials, 2006. **76**(2): p. 403-411.
42. Melo, L.P.d., et al., *Effect of injection molding melt temperatures on PLGA craniofacial plate properties during in vitro degradation.* International journal of biomaterials, 2017. **2017**(1): p. 1256537.
43. Kaith, B., et al., *Environment benevolent biodegradable polymers: Synthesis, biodegradability, and applications.* Cellulose Fibers: Bio-and Nano-Polymer Composites: Green Chemistry and Technology, 2011: p. 425-451.
44. Tamada, J. and R. Langer, *Erosion kinetics of hydrolytically degradable polymers.* Proceedings of the National Academy of Sciences, 1993. **90**(2): p. 552-556.
45. Go, A. and R. Langer, *Modeling monomer release from bioerodible polymers.* Journal of Controlled Release, 1995. **33**(1): p. 55-69.
46. Körber, M., *PLGA erosion: solubility-or diffusion-controlled?* Pharmaceutical research, 2010. **27**: p. 2414-2420.
47. Askadskii, A.A., et al., *The influence of the degree of crystallinity on the glass transition temperature of polymers.* Advanced Materials Research, 2014. **864**: p. 751-754.
48. Kost, B., et al., *The influence of the functional end groups on the properties of polylactide-based materials.* Progress in Polymer Science, 2022. **130**: p. 101556.
49. Machatschek, R. and A. Lendlein, *Fundamental insights in PLGA degradation from thin film studies.* Journal of controlled release, 2020. **319**: p. 276-284.

50. Hayashi, T., *Biodegradable polymers for biomedical uses.* Progress in polymer science, 1994. **19**(4): p. 663-702.
51. Weir, N., et al., *Degradation of poly-L-lactide. Part 1: in vitro and in vivo physiological temperature degradation.* Proceedings of the Institution of Mechanical Engineers, Part H: Journal of Engineering in Medicine, 2004. **218**(5): p. 307-319.
52. Vroman, I. and L. Tighzert, *Biodegradable polymers.* Materials, 2009. **2**(2): p. 307-344.
53. Li, S., H. Garreau, and M. Vert, *Structure-property relationships in the case of the degradation of massive poly (α-hydroxy acids) in aqueous media: Part 3 Influence of the morphology of poly (l-lactic acid).* Journal of Materials Science: Materials in Medicine, 1990. **1**(4): p. 198-206.
54. Hurrell, S. and R.E. Cameron, *Polyglycolide: degradation and drug release. Part I: changes in morphology during degradation.* Journal of Materials Science: Materials in Medicine, 2001. **12**: p. 811-816.
55. Kholodovych, V. and W.J. Welsh, *Densities of amorphous and crystalline polymers*, in *Physical properties of polymers handbook*. 2007, Springer. p. 611-617.
56. Van der Wal, A., J. Mulder, and R. Gaymans, *Fracture of polypropylene: The effect of crystallinity.* Polymer, 1998. **39**(22): p. 5477-5481.
57. Toft, M., *The effect of crystalline morphology on the glass transition and enthalpic relaxation in poly (ether-ether-ketone)*. 2012, University of Birmingham.
58. Park, J., et al., *Simultaneous measurement of glass-transition temperature and crystallinity of as-prepared polymeric films from restitution.* Macromolecules, 2021. **54**(20): p. 9532-9541.
59. Makadia, H.K. and S.J. Siegel, *Poly lactic-co-glycolic acid (PLGA) as biodegradable controlled drug delivery carrier.* Polymers, 2011. **3**(3): p. 1377-1397.
60. Chen, Z., et al., *Degradation behaviors of polylactic acid, polyglycolic acid, and their copolymer films in simulated marine environments.* Polymers, 2024. **16**(13): p. 1765.
61. Vazquez-Armendariz, J., et al., *Influence of controlled cooling on crystallinity of poly (L-lactic acid) scaffolds after hydrolytic degradation.* Materials, 2020. **13**(13): p. 2943.
62. Matveev, Y.I., V.Y. Grinberg, and V. Tolstoguzov, *The plasticizing effect of water on proteins, polysaccharides and their mixtures. Glassy state of biopolymers, food and seeds.* Food Hydrocolloids, 2000. **14**(5): p. 425-437.
63. Lu, Y., et al., *Properties of poly (lactic-co-glycolic acid) and progress of poly (lactic-co-glycolic acid)-based biodegradable materials in biomedical research.* Pharmaceuticals, 2023. **16**(3): p. 454.
64. Jain, S., et al., *Understanding of how the properties of medical grade lactide based copolymer scaffolds influence adipose tissue regeneration: Sterilization and a systematic in vitro assessment.* Materials Science and Engineering: C, 2021. **124**: p. 112020.
65. Vey, E., et al., *Degradation kinetics of poly (lactic-co-glycolic) acid block copolymer cast films in phosphate buffer solution as revealed by infrared and Raman spectroscopies.* Polymer degradation and stability, 2011. **96**(10): p. 1882-1889.
66. Eckel, F., et al., *Dependency of tensile properties and biodegradation on molecular mass during hydrolysis of poly (butylene succinate).* npj Materials Degradation, 2024. **8**(1): p. 97.
67. Huang, H., et al., *Room temperature brittle-to-ductile transition in polystyrene induced by extrusion casting melt stretching: Contribution of free volume and chain entanglement.* Polymer, 2024. **294**: p. 126745.
68. Masubuchi, Y., Y. Doi, and T. Uneyama, *Entanglement molecular weight.* Nihon Reoroji Gakkaishi, 2020. **48**(4): p. 177-183.
69. Liu, C., et al., *Evaluation of different methods for the determination of the plateau modulus and the entanglement molecular weight.* Polymer, 2006. **47**(13): p. 4461-4479.

70. Likhtman, A.E. and T.C. McLeish, *Quantitative theory for linear dynamics of linear entangled polymers.* Macromolecules, 2002. **35**(16): p. 6332-6343.
71. Pannuzzo, M., et al., *Predicting the miscibility and rigidity of poly (lactic-co-glycolic acid)/polyethylene glycol blends via molecular dynamics simulations.* Macromolecules, 2020. **53**(10): p. 3643-3654.
72. Shmool, T.A. and J.A. Zeitler, *Insights into the Structural Dynamics of PLGA at Terahertz Frequencies.* 2018.
73. Karatrantos, A., et al., *Modeling of entangled polymer diffusion in melts and nanocomposites: A review.* Polymers, 2019. **11**(5): p. 876.
74. Kumar, R., et al., *Harnessing autocatalytic reactions in polymerization and depolymerization.* MRS Communications, 2021. **11**: p. 377-390.
75. Hoy, R.S. and M.O. Robbins, *Strain hardening of polymer glasses: Effect of entanglement density, temperature, and rate.* Journal of Polymer Science Part B: Polymer Physics, 2006. **44**(24): p. 3487-3500.
76. Xu, D. and S.L. Craig, *Strain hardening and strain softening of reversibly cross-linked supramolecular polymer networks.* Macromolecules, 2011. **44**(18): p. 7478-7488.